Food Chemistry: X 35 (2026) 103757

Contents lists available at ScienceDirect

Food Chemistry: X

journal homepage: www.sciencedirect.com/journal/food-chemistry-x

The effects of exogenous spermidine on starch development, multi-scale structure, and in vitro digestibility in wheat were investigated under drought stress

Jialu Wen[a], Jianli Liu[a], Jianping Tang[a], Ting Zou[a], Aqing Gao[a], Vinay Nangia[b], Yang Liu[a,*]

[a] College of Agronomy/State Key Laboratory for Crop Stress Resistance and High-Efficiency Production, Northwest A&F University, Northwest A&F University, Yangling 712100, China

[b] International Center for Agricultural Research in the Dry Areas, Rabat 999055, Morocco

ARTICLE INFO

Keywords:
Wheat
Starch
Spermidine
Drought
Multi-scale structure

ABSTRACT

Spermidine (Spd) is a naturally occurring polyamine widely present in cereal grains. Despite its well-documented physiological activity in stress responses, whether Spd can directly regulate the multi-scale structure and digestive properties of wheat starch under drought conditions remains unclear. Therefore, this study applied drought stress (DR) during the early grain filling stage (1–10 days after anthesis), combined with exogenous spermidine spraying and spermidine inhibitor (Mitoguazone, MGBG), to investigate the effects of Spd on wheat starch formation, accumulation, multi-scale structure, and in vitro digestibility under DR treatment. The results showed that exogenous Spd enhanced starch synthase activity under DR treatment, promoted starch development and accumulation, and thereby increased wheat yield. Additionally, Spd increased the proportion of B-type starch granules, solubility, and swelling power under DR conditions. By reducing the proportion of long branched-chains, Spd decreased starch crystallinity and ordered structure, leading to lower gelatinization enthalpy and gelatinization temperature, while increasing the contents of rapidly digestible starch (RDS) and resistant starch (RS). In contrast, MGBG exhibited the opposite trends. This study reveals a novel function of polyamine compounds as starch structure modifiers, providing a chemical perspective for the quality regulation of food raw materials.

1. Introduction

Wheat is often exposed to variable adverse conditions, which typically lead to reduced crop productivity (Gu et al., 2025). Specifically, the grain-filling stage of wheat is sensitive to drought and susceptible to impacts from climate change (Ru et al., 2024). Yield losses induced by drought are considered one of the most significant damages to agricultural production (Van Hautegem et al., 2025). Therefore, enhancing the drought resistance of wheat during the grain-filling process is crucial for maintaining food security under future climate change.

Drought stress reduces the transport of carbohydrates from source organs, decreases the activity of starch synthases in wheat grains, and lowers starch content, leading to poor grain development and reduced grain weight (Li, Mao, et al., 2025). Starch, the primary component of wheat grains, is composed of two polymeric forms, amylose and amylopectin, and accounts for 60–75% of the grain's dry weight. The content and structure of starch determine its gelatinization and retrogradation properties, directly influencing the quality and stability of starch-based products (Qiu et al., 2025). The physicochemical properties and granule size distribution of wheat starch are controlled by both genetic and environmental factors. Post-anthesis water deficit reduces the volume and surface area percentage of B-type starch granules (Lu et al., 2014), while also diminishing starch binding capacity and gelatinization performance (Li et al., 2015). Furthermore, drought increases the content of RDS and RS, affecting the in vitro digestibility of starch (Yu et al., 2016). These findings indicate that drought affects starch formation and quality, yet its impact on wheat starch, particularly its multi-scale structure, requires further investigation.

The multi-scale structure of starch, which encompasses chain length distribution, crystallinity, ordered structure, and granule morphology, is closely associated with its physicochemical properties and its in vitro digestibility (Wen, Tang, et al., 2024), representing a research hotspot in

* Corresponding author.
E-mail address: yangl@nwafu.edu.cn (Y. Liu).

https://doi.org/10.1016/j.fochx.2026.103757
Received 29 December 2025; Received in revised form 28 February 2026; Accepted 12 March 2026
Available online 21 March 2026

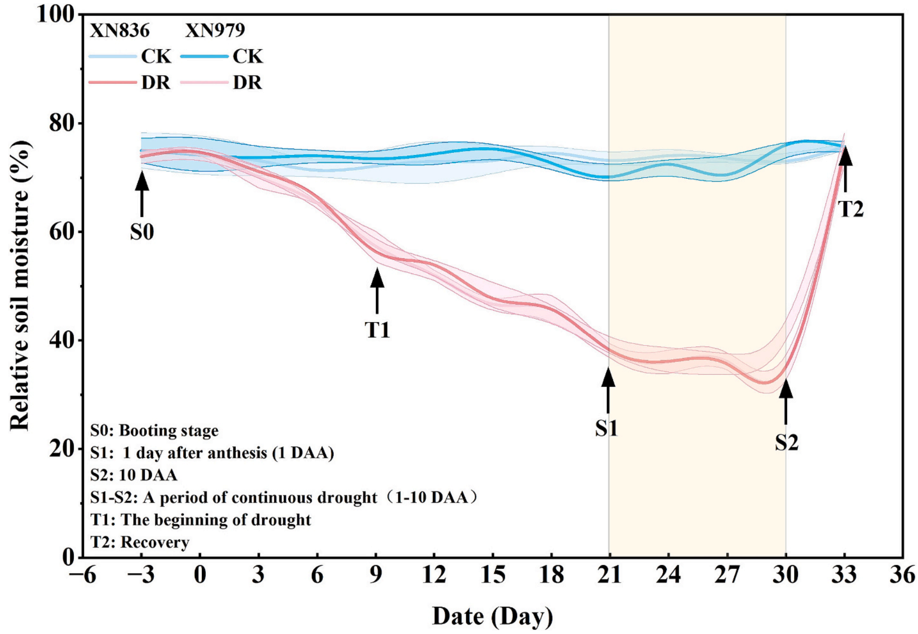

Fig. 1. Soil desiccation process from late booting stage to early grain filling stage (1–10 days post-anthesis).
CK: Normal moisture (70%–75% soil relative humidity). DR: Severe drought stress (35%–40% soil relative humidity). Data were collected from three replicate plots. The lines represent mean values, and the shaded areas represent the 95% confidence intervals.

the field of food chemistry. In plants, spermidine (Spd) functions not only as a growth regulator but has also been demonstrated to participate in the regulation of starch biosynthesis during wheat grain filling. Previous studies have shown that exogenous Spd modulates starch accumulation in cereal crops under stress conditions. For instance, under drought stress, Spd treatment significantly alters the amylose-to-amylopectin ratio in wheat endosperm and promotes the formation of B-type starch granules (Li et al., 2020; Yang et al., 2014). These findings suggest that Spd, as a chemical signal, can intervene in starch synthase activities, thereby remodeling the molecular structure and granular morphology of starch. However, existing research has primarily focused on yield and stress tolerance within the agronomic context, and systematic elucidation of how drought-induced molecular structural rearrangements mediated by exogenous Spd further influence the multi-scale structure and in vitro digestive properties of starch remains lacking. Therefore, investigating the regulatory mechanism of Spd on the multi-scale structure and digestive performance of wheat starch is of great significance for understanding the quality formation of cereal-based foods under adverse conditions.

Based on this, two wheat cultivars, XN836 (drought-insensitive) and XN979 (drought-sensitive), were used in this study. Drought treatment was applied during the early grain filling stage (1–10 days after anthesis). After 10 days of drought stress, water was replenished to normal field capacity until maturity. This research primarily aims to determine whether exogenous spermidine application can simultaneously increase grain weight and improve wheat starch quality. This study aims to elucidate, from a cereal chemistry perspective, the effects of exogenous spermidine on the multi-scale structure and in vitro digestive properties of wheat starch. The findings seek to reveal the potential of spermidine to improve the processing suitability and nutritional quality of starch-based foods through its regulation of starch accumulation processes, thereby providing theoretical support for stabilizing wheat starch quality in the context of climate change.

2. Materials and methods

2.1. Experimental site

The experiment was conducted from October 2024 to June 2025 in a rainout shelter (78 m × 18 m) at the Smart Agriculture Valley in Yangling District, Shaanxi Province (34°15′N, 108°02′E). The sides of the shelter remained open up to 1.5 m above the ground, and the roof was closed only during rainfall events to maintain ambient temperature conditions consistent with the outside environment. The site is located in the Guanzhong Plain, with the experimental field soil classified as Lou soil (cumulic cinnamonic). Prior to sowing, the baseline soil fertility in the 0–20 cm layer was as follows: available nitrogen, 52.32 mg kg^{-1}; available phosphorus, 22.46 mg kg^{-1}; available potassium, 115.47 mg kg^{-1}; and organic matter, 14.89 g kg^{-1}.

2.2. Experimental design

The experimental materials consisted of two wheat cultivars, XN836 (drought-insensitive) and XN979 (drought-sensitive), which were selected based on preliminary screening (Wen et al., 2026). These cultivars were approved by the Shaanxi Provincial and National Variety Committees in 2019 and 2009, respectively. The experiment was sown on 20 October 2024 and harvested on 29 May 2025. Management practices, including pest, disease, and weed control, were consistent with local conventional field practices.

Four experimental treatments were established: a well-watered control (CK, soil relative moisture 70–75%), drought stress (DR, soil relative moisture 35–40%), drought stress with exogenous spermidine application (DR + Spd), and drought stress with spermidine inhibitor application (DR + MGBG). Specifically, the treatments were: well-watered + water spraying (CK); drought stress + water spraying (DR); drought stress + spermidine spraying (DR + Spd); and drought + MGBG spraying (DR + MGBG).

Water control was initiated from the booting stage (Fig. 1). Soil moisture began to differ at the heading stage (T1), and significant differences emerged at the early grain-filling stage (S1, 1 day after anthesis). Drought stress was imposed during the early grain-filling stage (1–10 days after anthesis) for a duration of 10 days. After the drought period, all treatments were re-watered to maintain well-watered conditions (soil relative moisture 70–75%) until maturity.

Exogenous spermidine and its inhibitor were applied at the onset of drought stress, anthesis, and 10 days after anthesis. Applications were conducted on three consecutive days between 16:00 and 18:00 on clear days. The concentrations of Spd and MGBG were 1 mmol L^{-1} and 5 mmol L^{-1}, respectively, based on previous experiments from our research group (Li et al., 2020; Li, Li, Li, et al., 2024; Liu et al., 2016). To enhance adhesion, 0.1% Tween-20 was added to the spray solutions. The optimal application was determined when the solution adhered to the leaves without dripping, with a spray volume of 225 L per 225 m^2. Spd was purchased from Shanghai Macklin Biochemical Technology Co., Ltd. (China), and MGBG was obtained from Chengdu Yaomi Technology Co., Ltd. (China).

The experiment followed a split-plot design with two factors and three replicates. Each plot area was 6 m^2. Different water treatments were separated by a 2-m buffer. Soil volumetric water content in the 0–100 cm profile was measured every three days using an AZS-100 timed-position TDR soil moisture instrument (Beijing Ao Zuo Ecological Instrument Co., Ltd.), and soil relative moisture (0–60 cm in this study) was calculated. When soil volumetric water content approached the threshold, supplemental irrigation was applied based on calculations according to Sidika et al. (2012). Diammonium phosphate and urea were applied once as base fertilizer before sowing (without potassium fertilizer), providing a total of 180 kg N ha^{-1} and 120 kg P_2O_5 ha^{-1}.

2.3. Measurements and methods

2.3.1. Endosperm development

Wheat plants that flowered on the same day were selected and tagged at anthesis. Fresh grains were collected at 10 and 15 days post-anthesis (DPA), corresponding to the end of the drought period, and 5 days after rewatering, respectively. The samples were fixed in FAA solution and processed according to Yang, Wei, et al. (2024). The procedure included washing, dehydration, infiltration, embedding, and staining. Stained sections were imaged using a stereomicroscope (SZX–16; Olympus, Tokyo, Japan).

2.3.2. Starch-synthesizing enzymes and starch content

Fresh grains were sampled at 10, 15, and 20 DPA, rinsed with pre-cooled phosphate buffer (0.01 M, pH 7.4), and divided for separate analyses. For enzyme assays, a portion was homogenized on ice with phosphate-buffered saline (PBS) at a 1:9 (*w/v*) ratio. The homogenate was centrifuged at 5000 ×*g* for 10 min, and the supernatant was collected. The activities of ADP-glucose pyrophosphorylase (AGPase), granule-bound starch synthase (GBSS), soluble starch synthase (SSS), and starch branching enzyme (SBE) were determined using ELISA kits (Shanghai Kexing Trading Co., Ltd) via the double-antibody sandwich method, with absorbance measured at 450 nm. Another portion of grains was oven-dried for the determination of amylose, amylopectin, and total starch contents, following the method of Wen et al. (2024b).

2.3.3. Grain yield and its components

At maturity, 20 uniform and representative wheat spikes were selected to determine the kernel number per spike. A 1 m^2 area was harvested to count the spike number per square meter. The grains were sun-dried, and the thousand-kernel weight (TKW) was measured. The theoretical yield was calculated based on a grain moisture content of 13%.

2.3.4. Starch purification

Starch was isolated from flour using a dough washing method. Briefly, 150 g of flour was mixed with deionized water and kneaded into dough. The starch slurry was centrifuged at 3500 ×*g* for 10 min. The upper gray layer (mainly protein) was scraped off, and the remaining starch was resuspended in deionized water. This purification cycle was repeated three times. A final wash with absolute ethanol was performed to remove residual proteins. The purified starch was oven-dried at 40 °C and stored at 4 °C for subsequent analysis.

2.3.5. Starch color

The color parameters (L, a, b*) of starch samples were measured using a colorimeter (CS-820, Hangzhou, China).

2.3.6. Starch granule size distribution

Starch granule size distribution was analyzed using a laser diffraction particle size analyser. Samples were dispersed in deionized water and ultrasonicated for 30 s prior to measurement. The refractive indices were set at 1.33 for water and 1.53 for starch. The D10, D50, and D90 values were recorded (starch granules accumulated to the critical value of 10%, 50%, 90%).

2.3.7. Solubility, swelling power, and water solubility index

These properties were determined according to Gao et al. (2024). Wheat starch (2 g, Wo) was dispersed in a 50 mL centrifuge tube containing 20 mL of distilled water. The mixture was then heated (90 °C, 15 min), cooled to room temperature (25 °C), and centrifuged (4000 ×*g*, 10 min). The supernatant was poured into a pre-weighed evaporation dish for determination of solid content, and the sediment was weighed (Ws). The supernatant was dried overnight at 105 °C to obtain the weight of dried solids (Wd). Solubility, water solubility index (WSI), and swelling power (SP) were calculated using the following formulas:

Solubility (g/g) = Ws/Wo

WSI (%) = (Wd/Wo) × 100

SP (g/g) = Ws/(Wo-Wd).

2.3.8. Starch chain length distribution

The chain length distribution of amylopectin was analyzed by high-performance anion-exchange chromatography with pulsed amperometric detection (HPAEC-PAD) using a CarboPac PA-200 column on a Dionex ICS 5000 system. Technical support was provided by Sanshu Biotechnology Co., Ltd. (Shanghai, China).

2.3.9. Starch crystallinity

The crystalline structure and relative crystallinity of the starch samples were analyzed using an X-ray diffractometer (Bruker D8 Advance, Germany). The operating conditions were: voltage 40 kV, current 40 mA, scanning range from 5° to 50° (2θ), and a scanning speed of 10° min^{-1}. The relative crystallinity was calculated from the diffraction patterns using JADE 6.0 software.

2.3.10. Fourier transform infrared spectroscopy

The short-range molecular order of starch was analyzed by FTIR spectroscopy. Starch samples were mixed with potassium bromide (KBr) at a 1:100 (*w*/w) ratio and pressed into pellets. Spectra were collected over the wavenumber range of 4000–400 cm^{-1} with 32 scans using an FTIR spectrometer (Thermo Fisher, USA). The deconvolution of the spectra was performed using Peak Fit 4.0 software (Ni et al., 2025).

2.3.11. Rapid visco analysis

Starch pasting properties were measured using a Rapid Visco Analyser (Perten, TechMaster, Sweden). Starch (3 g, dry basis) was mixed with 25 mL of distilled water in an RVA canister. The slurry was homogenized using the RVA paddle, and the standard heating-cooling profile was run.

2.3.12. Thermal properties

Starch samples (3 mg) were weighed into aluminum pans, mixed with 9 μL of deionized water, and hermetically sealed. The sealed pans were then equilibrated at 4 °C for 24 h. The thermal properties of the starch were analyzed using a differential scanning calorimeter (DSC, TA

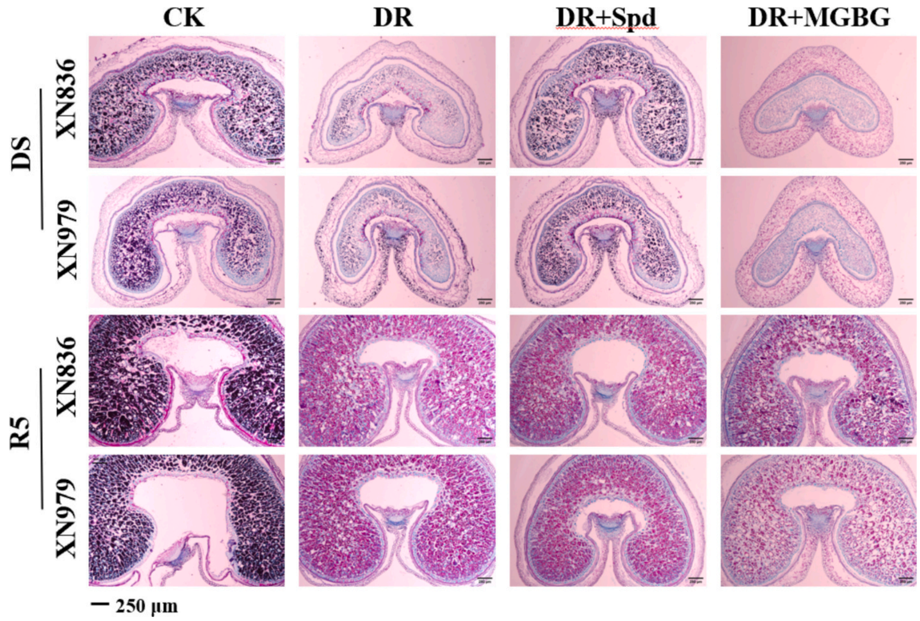

Fig. 2. Endosperm development of wheat grains under different treatments during grain filling.
DS: Drought stress for 10 days. R5: Rehydration for 5 days. Bar = 250 μm.

Instruments, USA). The samples were heated from 25 to 90 °C at a rate of 10 °C min^{-1}. The onset (To), peak (Tp), and conclusion (Tc) temperatures, as well as the gelatinization enthalpy (ΔH), were recorded (Li & Zhu, 2018).

2.3.13. In vitro digestibility

The in vitro digestibility of starch was determined according to Wen et al. (2024). Starch was dispersed in distilled water, gelatinized in a boiling water bath for 30 min, and then equilibrated at 37 °C. Enzymatic hydrolysis was initiated, and aliquots (0.1 mL) were taken at 0, 20, and 120 min. The reaction was terminated by adding absolute ethanol, followed by centrifugation. The glucose content in the supernatant was quantified using a GOPOD assay kit (Megazyme), and the contents of rapidly digestible starch (RDS), slowly digestible starch (SDS), and resistant starch (RS) were calculated.

2.4. Data analysis

All data represent means ± standard deviation of three replicates. Conduct a preliminary analysis by Microsoft EXCEL. Data were subjected to a two-way analysis of variance (ANOVA) with cultivar and treatment as fixed factors. Significant differences among treatment means were determined by the Least Significant Difference (LSD) test at the $P < 0.05$ level. Figures were prepared using Origin 2025 and Microsoft PowerPoint 2021.

3. Results

3.1. Wheat yield components

The drought stress (DR) treatment significantly reduced the kernel number per spike and the thousand-kernel weight (1000-grain weight, TKW), whereas the number of spikes per unit area remained largely unaffected (Fig. S1). Compared to the well-watered control (CK), the DR treatment decreased the kernel number per spike by 5.09% in XN836 and 6.30% in XN979. The TKW was reduced by 5.08% and 9.20% in XN836 and XN979, respectively. Consequently, the final grain yield under DR declined by 10.42% for XN836 and 15.26% for XN979. Exogenous spermidine application (DR + Spd) effectively mitigated the negative impact of DR on grain weight. Compared to the DR treatment alone, DR + Spd significantly increased the TKW by 7.08% in XN836 and 4.78% in XN979, and also elevated the kernel number per spike. These results demonstrate that exogenous Spd can alleviate the decline in TKW induced by drought stress, thereby promoting yield recovery. In contrast, the application of the Spd biosynthesis inhibitor MGBG (DR + MGBG) exacerbated the reduction in these yield components.

3.2. Endosperm cell development process

The endosperm cells develop along with the grain filling process, and the endosperm cells are gradually filled by the grains (Fig. 2). During the early grain-filling stage (1–10 days after anthesis, DPA), DR inhibited the division of endosperm cells in both varieties, resulting in smaller grain morphogenesis, while exogenous Spd alleviated the development of wheat endosperm cells under DR treatment. On the 15th day of the grain-filling period (5 days after rewatering, R5), DR hindered the development of endosperm cells (with more blank gaps and less plump grains), whereas exogenous Spd further mitigated the damage caused by DR to the wheat endosperm. MBGB led to delayed endosperm development or smaller grains.

3.3. Changes in key starch synthesizing enzyme

Application of exogenous spermidine significantly affected the abundance of starch synthesis-related enzyme proteins in wheat grains. The protein levels of these enzymes exhibited a trend of initially increasing and then decreasing throughout the grain-filling process, peaking at the R5 stage (Fig. 3 A-D). During the DS stage, compared with the CK treatment, the DR treatment significantly reduced the protein levels of AGPase, GBSS, SBE, and SSS in grains of both XN836 and XN979, with decreases of 12.58%, 12.20%, 20.67%, 10.72%, 26.91%, 13.96%, 34.70%, and 24.76%, respectively. Notably, the magnitude of reduction in starch synthesis-related enzyme proteins under DR treatment was substantially greater in XN979 grains than in XN836 grains compared to CK, indicating that XN979 is more sensitive to drought stress. Compared with the DR treatment, the DR + Spd treatment significantly increased the levels of these enzyme proteins in grains, with increments of 15.75%, 5.38%, 28.61%, 11.88%, 14.74%, 4.39%, 25.61%, and 9.14%, respectively. However, in the DR + MGBG treatment, MGBG further inhibited the accumulation of enzyme proteins

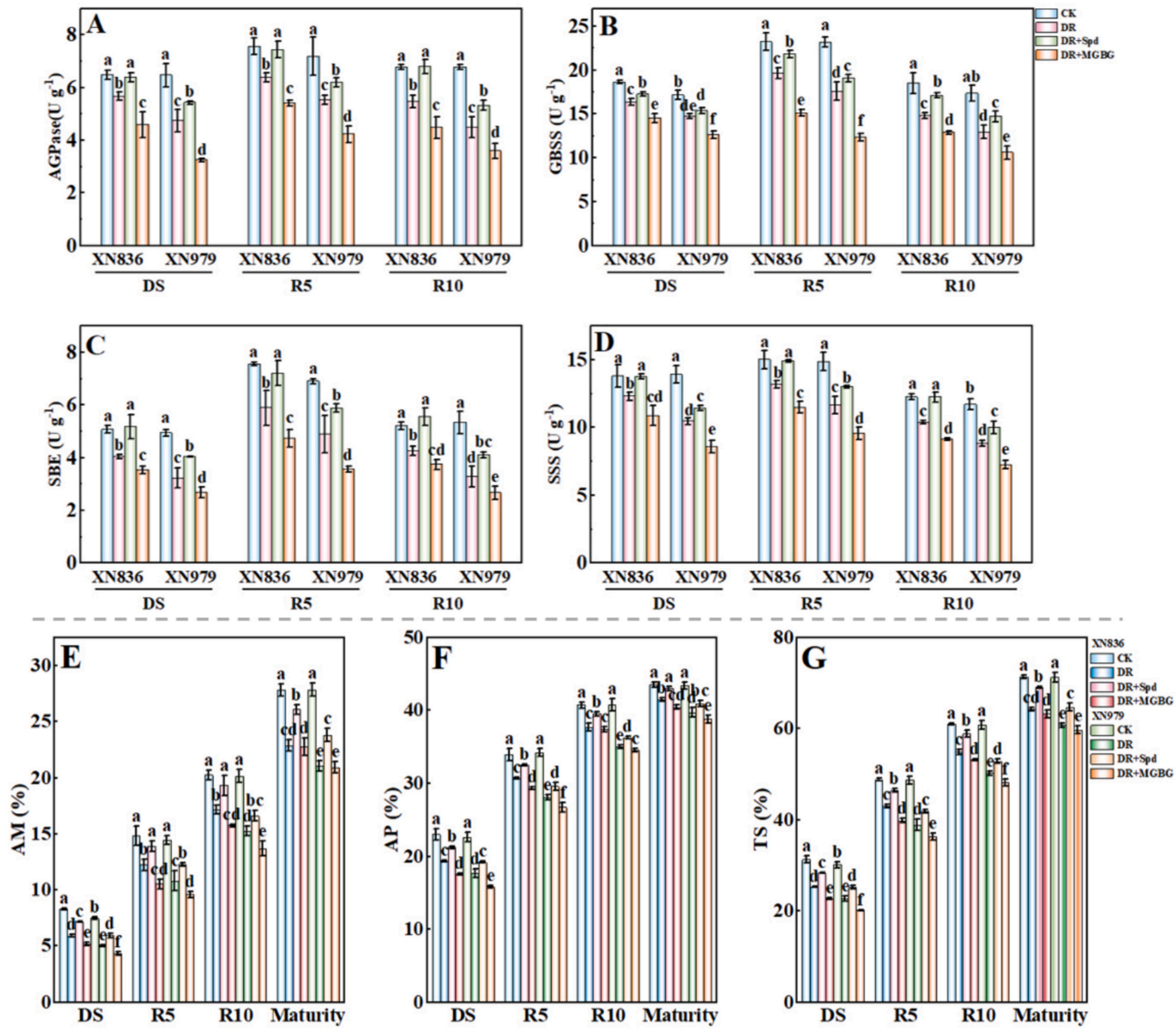

Fig. 3. Effects of exogenous spermidine on starch synthase and starch content in wheat grain under post-anthesis drought stress.
DS: Drought stress for 10 days. R5: Rehydration for 5 days. R10: Rehydration for 10 days. A: ADP-glucose pyrophosphorylase (AGPase). B: Granule-bound starch synthase (GBSS). C: Soluble starch synthase (SSS). D: Starch branching enzyme (SBE). E: Amylose content (AM). F: Amylopectin content (AP). G: Total starch content (TS). All data represent means ± standard deviation of three replicates. There were significant differences in the values of different letters in the same column ($P < 0.05$).

relative to DR, even showing a significant decreasing trend.

At the R5 stage, compared with CK, DR still significantly reduced enzyme protein levels, but Spd application increased the levels of related proteins under the DR + Spd treatment. This suggests that the damage caused by drought stress to wheat persists even after rewatering. The trends observed at the R10 stage were generally consistent with those at R5.

These results indicate that drought stress reduces the protein abundance of AGPase, GBSS, SBE, and SSS, which may consequently inhibit starch synthesis in wheat grains. However, Spd application effectively improved the levels of starch synthesis-related enzyme proteins in grains under drought stress (particularly in XN836), whereas MGBG exhibited an inhibitory effect.

3.4. Dynamic changes in starch components

The contents of amylose (AM), amylopectin (AP), and total starch (TS) in wheat grains increased progressively during grain development, peaking at maturity across all treatments. The overall order of content was consistently: CK > DR + Spd > DR > DR + MGBG (Fig. 3 *E*-G). At the DS stage, the drought stress (DR) treatment significantly reduced the accumulation of AM, AP, and TS compared to the CK. The inhibition was more severe in the drought-sensitive cultivar XN979 than in the drought-insensitive XN836. Exogenous spermidine application (DR + Spd) effectively mitigated this reduction. At the DS stage, DR + Spd significantly increased the contents of AM, AP, and TS relative to the DR treatment alone. The most substantial increase was observed for AM in XN836 (21.32%). Conversely, the application of the Spd biosynthesis inhibitor MGBG (DR + MGBG) led to a further significant decrease in all starch components, with a more pronounced effect in XN979. Notably, the negative impact of the early drought stress persisted even after rewatering at the R5 stage. Compared to CK, the DR treatment still significantly suppressed the contents of AM, AP, and TS at R5, although the extent of reduction was smaller than that at the DS stage. This indicates that the physiological damage was not fully reversible upon rehydration. Meanwhile, the DR + Spd treatment maintained higher

Table 1
Effects of exogenous spermidine on starch granule size distribution and color of post-anthesis wheat under drought stress.

Variety	Treatment	0,10	0,50	0,90	A	B	L*	a*	b*
XN836	CK	7.57 ± 0.03a	17.57 ± 0.09b	26.45 ± 0.09b	76.40 ± 0.13 g	23.68 ± 0.05a	97.58 ± 0.06ab	−0.47 ± 0.001e	1.52 ± 0.02f
	DR	6.85 ± 0.01c	17.09 ± 0.03d	26.25 ± 0.03d	78.38 ± 0.10d	21.62 ± 0.40d	97.17 ± 0.09bc	−0.45 ± 0.005d	1.62 ± 0.02e
	DR + Spd	7.46 ± 0.09ab	18.56 ± 0.01a	26.90 ± 0.01a	77.56 ± 0.13e	22.44 ± 0.13c	97.99 ± 0.64a	−0.48 ± 0.002e	1.56 ± 0.03f
	DR + MGBG	6.10 ± 0.03e	16.60 ± 0.01f	26.07 ± 0.01f	79.46 ± 0.05b	20.54 ± 0.05f	97.16 ± 0.07c	−0.45 ± 0.010d	1.67 ± 0.03e
XN979	CK	7.27 ± 0.37b	17.41 ± 0.06c	26.45 ± 0.06c	76.94 ± 0.03f	23.06 ± 0.20b	97.91 ± 0.04a	−0.33 ± 0.006c	1.85 ± 0.04d
	DR	6.37 ± 0.05d	16.73 ± 0.03e	26.09 ± 0.03e	79.49 ± 0.01b	20.51 ± 0.22f	97.22 ± 0.10bc	−0.31 ± 0.002b	2.15 ± 0.04b
	DR + Spd	6.83 ± 0.08c	17.61 ± 0.03b	27.02 ± 0.03b	78.92 ± 0.05c	21.08 ± 0.05e	97.79 ± 0.06a	−0.32 ± 0.006c	1.98 ± 0.03c
	DR + MGBG	5.55 ± 0.06f	16.19 ± 0.07 g	25.81 ± 0.07 g	80.77 ± 0.09a	19.23 ± 0.10 g	97.04 ± 0.06c	−0.29 ± 0.021a	2.29 ± 0.04a
	V	**	**	ns	**	**	ns	**	**
ANOVA	T	**	**	**	**	**	**	**	**
	V*T	ns	**	ns	**	*	ns	ns	**

Note: CK: 70%–75% soil relative humidity. DR: 35%–40% soil relative humidity. XN836: Xinong 836. XN979: Xinong979. V: Variety. T: Treatment. $V \times T$: Interaction of varieties and treatments. 0, 1, 0, 50, 0, 90, starch granules accumulated to the critical value of 10%, 50%, 90%. A, A-type starch granules. B, B-type starch granules. L*: Brightness. a* and b*: chromaticity coordinates. * and ** indicate significance at the $P < 0.05$ and 0.01 levels, respectively, ns: not significant ($P > 0.05$). All data represent means ± standard deviation of three replicates. Different lowercase letters represent significant differences, $P < 0.05$.

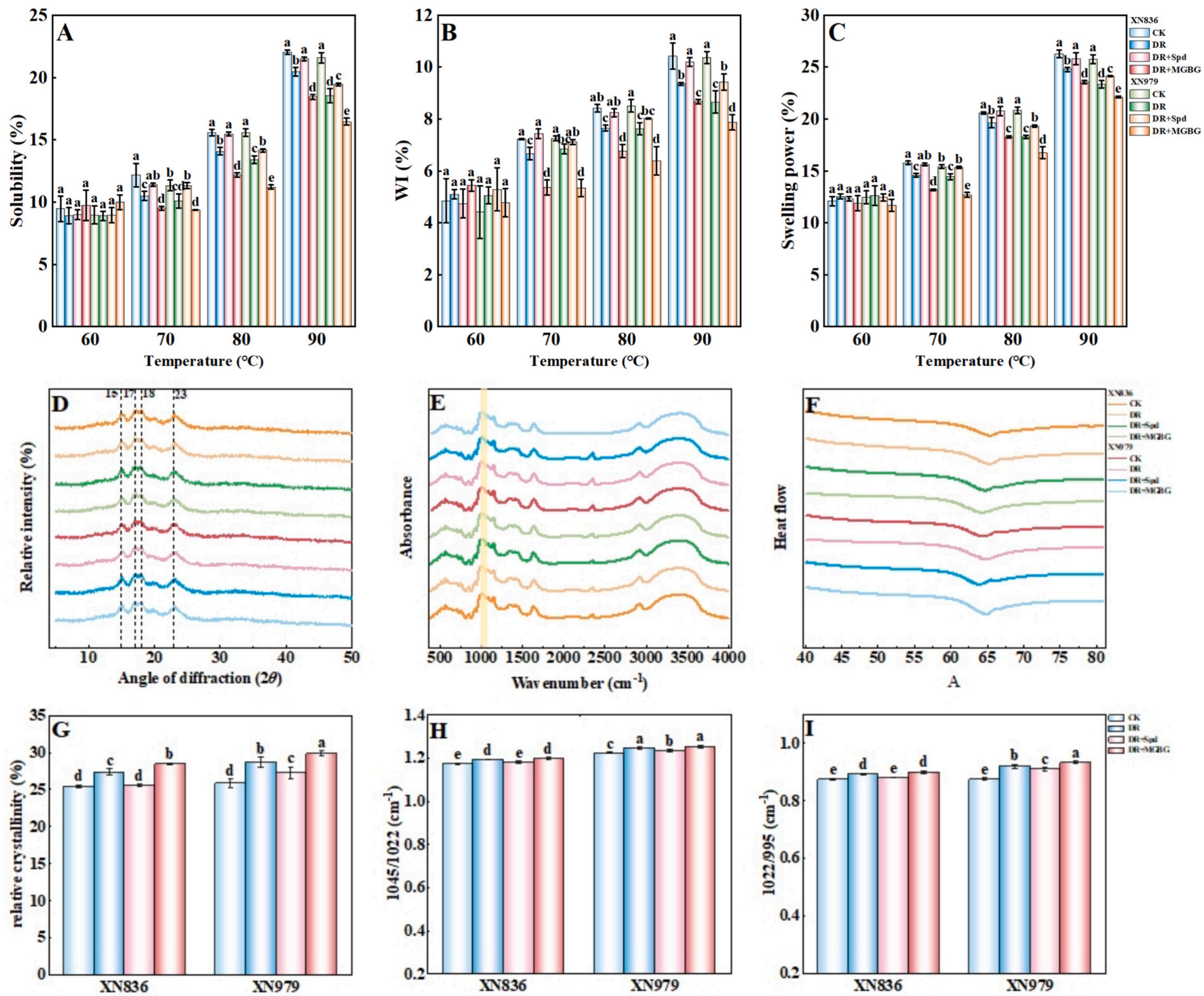

Fig. 4. Effects of exogenous spermidine on starch solubility, WSI, SP, crystallinity, DSC and FITR of wheat under drought stress after post-anthesis.
A: Solubility of starch. B: Water solubility index of starch. C: Swelling power of starch. D: Relative crystallinity map of starch. E: Fourier transforms infrared spectrum of starch. The yellow area C indicates the range between 990 and 1050. F: Thermal characteristic map (DSC). G: The relative crystallinity of starch. F: 1022/995 cm^{-1}. F:1047/1022 cm^{-1}. All data represent means ± standard deviation of three replicates. There were significant differences in the values of different letters in the same column ($P < 0.05$). (For interpretation of the references to color in this figure legend, the reader is referred to the web version of this article.)

starch contents compared to DR at this stage, demonstrating the sustained positive effect of Spd. These trends remained consistent at the 20th day of the grain-filling period (10 days after rewatering, R10) and maturity. In summary, the initial drought stress inflicted persistent damage, Spd effectively alleviated this inhibition and promoted starch synthesis under drought stress conditions, whereas the spermidine biosynthesis inhibitor MGBG exacerbated the negative effects.

3.5. Starch color parameters

The color parameters of starch from both cultivars under normal irrigation (CK) showed no significant differences (Table 1). However, DR significantly reduced the brightness (L*) and the chromaticity coordinates (a* and b*) compared to CK. Exogenous spermidine application (DR + Spd) effectively counteracted this decline, significantly increasing the L, a, and b* values relative to the DR treatment, bringing them closer to the CK levels. Conversely, the application of the Spd biosynthesis inhibitor MGBG (DR + MGBG) led to a further significant reduction in all color parameters, resulting in the darkest starch among all treatments.

3.6. Starch granule size distribution

The size distribution of wheat starch granules was significantly influenced by the treatments. The volume and surface area distributions displayed typical bimodal curves, whereas the number distribution was unimodal (Fig. S2). Although the overall profile of the distribution curves was consistent, the treatments markedly altered the granule size parameters and the proportion of different granule types. Compared to the CK, the DR treatment significantly reduced the starch granule size, as indicated by lower D10, D50, and D90 values in both cultivars, with the exception of D90 in XN836 (Fig. S2, Table 1). The drought-sensitive XN979 generally exhibited more substantial reductions. Exogenous spermidine application (DR + Spd) effectively reversed this trend induced by DR. The DR + Spd treatment significantly increased all granule size parameters (D10, D50, D90) in both cultivars compared to DR alone, resulting in larger granules. Conversely, the DR + MGBG treatment led to the smallest granule sizes among all treatments. We further categorized the granules into A-type (large) and B-type (small). The DR treatment increased the volume proportion of A-type granules while significantly decreasing that of B-type granules, with a more pronounced reduction in XN979 (−11.05%) than in XN836 (−8.69%). In contrast, the DR + Spd treatment significantly increased the proportion of B-type granules relative to the DR treatment. The DR + MGBG treatment further suppressed the development of B-type granules, showing an opposite trend to DR + Spd. In summary, drought stress promoted the formation of A-type granules at the expense of B-type granules and reduced overall granule size. Exogenous spermidine mitigated these effects by increasing granule size and the proportion of B-type granules under stress conditions, whereas the Spd biosynthesis inhibitor MGBG exacerbated the inhibition of starch granule development.

3.7. Swelling power and solubility properties of starch

The solubility, water solubility index (WSI), and swelling power of starch from all treatments increased with temperature, becoming discernible at 70 °C and reaching maxima at 90 °C (Fig. 4 A-C). At 90 °C, DR significantly impaired these functional properties compared to the CK. The drought-sensitive cultivar XN979 exhibited more substantial reductions than XN836. For instance, the WSI of XN979 decreased by 14.23%, compared to a 5.66% reduction in XN836 (Fig. 4 B). Exogenous spermidine application (DR + Spd) effectively mitigated the negative effects of DR. The DR + Spd treatment significantly enhanced the solubility, WI, and swelling power relative to the DR treatment alone, with increases ranging from 4.21% to 8.98% for XN836 and 3.39% to 8.89% for XN979. In contrast, the DR + MGBG treatment resulted in the lowest values for all three parameters. In conclusion, exogenous spermidine effectively ameliorated the solubility, WSI, and swelling power of wheat starch under drought stress.

Table 2
Effects of exogenous spermidine on the distribution of amylopectin chain length in wheat under drought stress after anthesis.

Variety	Treatment	DP 6–12	DP 13–24	DP 25–36	DP>37
XN836	CK	26.40 ± 0.014 cd	45.75 ± 0.099a	14.40 ± 0.028e	13.49 ± 0.007f
	DR	26.35 ± 0.029e	45.12 ± 0.057c	14.86 ± 0.019b	13.68 ± 0.010c
	DR + Spd	26.42 ± 0.007c	45.31 ± 0.010b	14.76 ± 0.011c	13.54 ± 0.007e
	DR + MGBG	26.34 ± 0.008e	45.05 ± 0.008c	14.93 ± 0.014a	13.68 ± 0.021c
XN979	CK	26.38 ± 0.021de	45.43 ± 0.007b	14.42 ± 0.013e	13.79 ± 0.014b
	DR	26.19 ± 0.008f	45.10 ± 0.071c	14.90 ± 0.003ab	13.84 ± 0.021a
	DR + Spd	26.53 ± 0.007a	45.31 ± 0.042b	14.67 ± 0.028d	13.50 ± 0.002f
	DR + MGBG	26.50 ± 0.007b	45.13 ± 0.007c	14.77 ± 0.007c	13.66 ± 0.007d
ANOVA	V	*	*	**	**
	T	**	**	**	**
	V*T	**	**	**	**

Note: CK: 70%–75% soil relative humidity. DR: 35%–40% soil relative humidity. XN836: Xinong 836. XN979: Xinong979. V: Variety. T: Treatment. V × T: Interaction of varieties and treatments. * and ** indicate significance at the $P < 0.05$ and 0.01 levels, respectively, ns: not significant ($P > 0.05$). All data represent means ± standard deviation of three replicates. Different lowercase letters represent significant differences, $P < 0.05$.

3.8. Amylopectin chain length distribution

The chain length distribution of amylopectin was significantly altered by the treatments (Table 2). Based on structural characteristics, chains were categorized as A (DP 6–12), B1 (DP 13–24), B2 (DP 25–36), and B3 (DP ≥37) (Pang et al., 2024). Compared to the CK, DR significantly reduced the proportion of short chains (A and B1) while increasing the proportion of long chains (B2 and B3). This indicates that DR stress promoted the synthesis of longer amylopectin chains. Exogenous spermidine application (DR + Spd) counteracted this DR-induced trend. Specifically, DR + Spd increased the proportion of short chains and decreased that of long chains relative to the DR treatment alone. In contrast, the DR + MGBG treatment resulted in a chain length distribution that was similar to, or even more pronounced than, the DR treatment. These findings demonstrate that drought stress favors the formation of longer amylopectin chains, whereas exogenous spermidine promotes a shorter-chain profile under such stress conditions.

3.9. Crystalline structure analyzed by X-ray diffraction

X-ray diffraction analysis revealed that all starch samples exhibited a typical A-type crystalline pattern, characterized by distinct peaks at 2θ of approximately 15°, 17°, 18°, and 23° (Fig. 4 D). This indicates that neither DR nor exogenous spermidine altered the fundamental crystal type. However, they significantly influenced the relative crystallinity. Compared to the CK, the DR treatment significantly increased the relative crystallinity by 7.71% in XN836 and 11.03% in XN979 (Fig. 4 G). Exogenous spermidine (DR + Spd) effectively counteracted this effect, significantly reducing the crystallinity relative to the DR treatment by 6.64% and 5.01% in XN836 and XN979, respectively. Conversely, the DR + MGBG treatment further increased the relative crystallinity.

Table 3
Effects of exogenous spermidine on the thermal properties of wheat starch after post-anthesis drought stress.

Variety	Treatment	To (°C)	Tp (°C)	Tc (°C)	ΔH ($J.g^{-1}$)
XN836	CK	57.39 ± 0.49d	60.35 ± 0.25ef	68.71 ± 0.38f	4.42 ± 0.09d
	DR	58.37 ± 0.13c	61.26 ± 0.05d	70.38 ± 0.53 cd	5.03 ± 0.41c
	DR + Spd	57.42 ± 0.16d	60.14 ± 0.60f	69.45 ± 0.44e	3.67 ± 0.35e
	DR + MGBG	58.73 ± 0.27c	61.64 ± 0.11 cd	71.60 ± 0.13b	5.17 ± 0.03c
XN979	CK	58.47 ± 0.07c	60.67 ± 0.12e	68.76 ± 0.12f	4.01 ± 0.06de
	DR	59.45 ± 0.29b	62.70 ± 0.14b	70.95 ± 0.20c	6.09 ± 0.18b
	DR + Spd	58.72 ± 0.09c	61.82 ± 0.12c	70.01 ± 0.45de	4.15 ± 0.09d
	DR + MGBG	60.33 ± 0.29a	63.24 ± 0.41a	72.41 ± 0.49a	6.62 ± 0.35a
ANOVA	V	**	**	**	**
	T	**	**	**	**
	V*T	ns	**	ns	**

Note: CK: 70%–75% soil relative humidity. DR: 35%–40% soil relative humidity. XN836: Xinong 836. XN979: Xinong 979. V: Variety. T: Treatment. V × T: Interaction of varieties and treatments. To: Onset temperature. Tp: Peak temperature. Tc: Conclusion temperature. ΔH: Gelatinization enthalpy. * and ** indicate significance at the $P < 0.05$ and 0.01 levels, respectively, ns: not significant ($P > 0.05$). All data represent means ± standard deviation of three replicates. Different lowercase letters represent significant differences, $P < 0.05$.

3.10. Fourier transform infrared spectroscopy

The FTIR spectra were consistent across all treatments, confirming that no new chemical groups were introduced (Fig. 4 E). To quantify changes in the short-range molecular order, the ratios of absorbance at specific wavenumbers were calculated. The ratio R_1 (1045/1022 cm^{-1}) reflects the degree of ordered structure, while R_2 (1022/995 cm^{-1}) is related to the amorphous content. Compared to CK, the DR treatment significantly increased both the R_1 and R_2 ratios (Fig. 4 H, Fig. 4 I), indicating an enhancement in the short-range structural order. This effect was more pronounced in XN979. In contrast, the DR + Spd treatment significantly reduced these ratios compared to DR alone, suggesting that spermidine degraded the double-helical order within the starch. The DR + MGBG treatment further increased the R_1 and R_2 ratios. In summary, drought stress increased the structural order of wheat starch at both the crystalline (long-range) and double-helical (short-range) levels. Exogenous spermidine effectively disrupted this stress-induced ordering, while the spermidine biosynthesis inhibitor MGBG had the opposite effect.

3.11. Pasting and thermal properties of starch

The pasting properties of wheat starch, as determined by Rapid Visco Analyser (RVA), were significantly influenced by the treatments (Table 4). Compared to the CK, the DR treatment significantly reduced the peak viscosity (PV), trough viscosity (TV), and final viscosity (FV) in both cultivars, with the drought-sensitive XN979 exhibiting greater reductions (TV: −10.72%) than XN836 (TV: −3.85%). Conversely, DR increased the breakdown (BD), setback (SB), and pasting temperature (PT). Exogenous spermidine application (DR + Spd) effectively ameliorated these alterations. Compared to DR alone, DR + Spd significantly increased PV, TV, and FV while decreasing BD, SB, and PT. In contrast, the DR + MGBG treatment further deteriorated the pasting quality, resulting in the lowest viscosity parameters.

The thermal properties during gelatinization were analyzed using Differential Scanning Calorimetry (DSC) (Fig. 4 F, Table 3). All samples displayed a major endothermic transition near 65 °C. Compared to CK, the DR treatment significantly increased the onset (To), peak (Tp), and conclusion (Tc) temperatures, as well as the gelatinization enthalpy (ΔH). The increase in ΔH was particularly pronounced in XN979 (51.79%), indicating a substantially higher energy requirement to disrupt the more ordered molecular structure formed under stress. The DR + Spd treatment counteracted this effect, significantly reducing To, Tp, Tc, and ΔH compared to DR alone. The DR + MGBG treatment resulted in the highest ΔH values among all treatments for each cultivar. Statistical analysis indicated that while both cultivar and treatment significantly affected all thermal parameters, their interaction did not have a significant effect on To and Tc ($P > 0.05$), suggesting that the main effects of cultivar and treatment were dominant for these parameters.

3.12. In vitro starch digestibility

The in vitro digestibility of starch was significantly modulated by the treatments (Fig. 5). Compared to the CK, the DR treatment markedly increased the content of RDS and decreased the contents of SDS and RS. These shifts were more pronounced in the drought-sensitive cultivar XN979 (RDS: +17.20%; RS: −10.12%) than in XN836 (RDS: +11.32%; RS: −5.68%). Exogenous spermidine application (DR + Spd) effectively counteracted the DR-induced changes in digestibility. Specifically, DR + Spd significantly reduced the RDS content and increased the SDS and RS contents relative to the DR treatment alone. In contrast, the DR + MGBG treatment further reduced the SDS and RS contents, resulting in

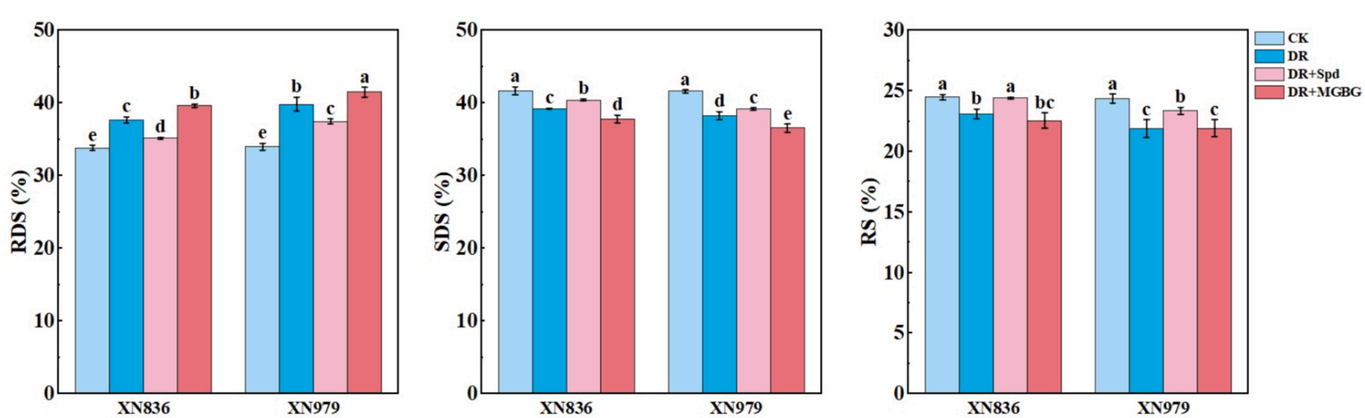

Fig. 5. Effects of exogenous spermidine on in vitro digestion of wheat starch after post-anthesis rewatering under drought stress.
RDS: rapidly digestible starch. SDS: slowly digestible starch. RS: resistant starch. All data represent means ± standard deviation of three replicates. There were significant differences in the values of different letters in the same column ($P < 0.05$).

the least desirable nutritional profile. These results demonstrate that exogenous spermidine can improve the nutritional quality of wheat starch under drought stress by promoting the formation of SDS and RS over RDS.

4. Discussion

4.1. Exogenous spermidine promotes starch development and accumulation under drought stress

The grain-filling period is a critical phase for wheat grain weight determination, during which drought stress inevitably leads to yield reduction. In this study, DR applied at the early grain-filling stage decreased the number of grains per spike and the TKW, with a more pronounced reduction observed in XN979 (Fig. S1). Starch constitutes a major component of wheat grains, and its biosynthesis and accumulation are influenced by external environmental factors. For instance, previous studies have demonstrated that water deficit during grain filling leads to reduced activities of starch synthases and lower starch content in wheat (Li et al., 2020). Consistent with this, the present study found that DR treatment significantly inhibited the protein abundance (determined by ELISA) of key starch synthesis enzymes including AGPase, SSS, GBSS, and SBE in wheat grains, and ultimately reduced the contents of total starch, amylose, and amylopectin (Fig. 3). Endosperm development is a crucial event in wheat seed development and is highly sensitive to environmental conditions. The results of this study indicate that wheat endosperm development is highly sensitive to DR, resulting in delayed cellular differentiation (Fig. 2), This provides a cellular-level explanation for the decline in starch synthesis capacity.

Application of exogenous Spd effectively reversed the negative effects caused by DR treatment. Exogenous Spd promoted the accumulation of starch granules within amyloplasts in the endosperm under DR conditions (Fig. 2), enhanced the protein abundance of key starch-synthesizing enzymes, increased starch content (Fig. 3), and elevated TKW (Fig. S1). This improvement can be attributed to several factors: (1) Spd increased chlorophyll content in wheat leaves under DR, thereby enhancing photosynthetic capacity and supplying more adequate photoassimilates for grain development (Li, Liang, Li, et al., 2024; Liu et al., 2025). (2) Spd strengthened the antioxidant defense system in wheat, maintained cellular homeostasis, and facilitated the translocation of carbohydrates to the grains (Li, Liang, Feng, et al., 2024). (3) Within the grains we observed that exogenous Spd restored the normal pattern of endosperm cell division and differentiation under DR conditions (Fig. 2), significantly increased the protein abundance of key starch synthesis enzymes (Fig. 3), and ultimately promoted starch accumulation in endosperm cells (Fig. 2), leading to enhanced grain weight. This series of promoting effects was abolished or even reversed upon application of the spermidine synthesis inhibitor MGBG, further confirming the specific regulatory role of Spd.

4.2. Spermidine regulates starch granule distribution under severe drought stress and improves the multi-scale structure of wheat starch

Starch granule distribution is a key parameter influencing starch functionality, directly affecting the textural properties of flour-based products (Li et al., 2025). DR reduced the proportion of A-type starch granules while increasing that of B-type granules (Table 1). This is attributed to the developmental timing: A-type granules initiate formation around 4–5 days after anthesis, whereas B-type granules begin developing approximately 8 days post-anthesis. In this experiment, the persistent severe drought stress occurred during the early grain-filling stage (1–10 days), which likely restricted the formation of B-type granules, potentially diverting available substrates to A-type granules which aligns with findings from previous research (Yang et al., 2014). This effect may stem from Spd delaying leaf senescence and prolonging the grain-filling period in wheat, allowing more time for the development of smaller B-type granules during the rehydration phase post-day 10 (Liu et al., 2013; Liu et al., 2016; Xu et al., 2016) , this provided more sufficient time for the formation and development of B-type starch granules during the middle and late grain-filling stages. The increased proportion of B-type granules explains why the whiteness index of starch was significantly elevated under DR + Spd treatment (Table 1), as smaller granules exhibit stronger light scattering, resulting in a whiter appearance of the starch. Meanwhile, Spd reversed the DR-induced decreases in particle size D (0.1), D (0.5), and D (0.9). This indicates that exogenous Spd participates in shaping granule size distribution potentially by enhancing the protein abundance of key starch-synthesizing enzymes (Fig. 3) or modulating gene expression, thereby increasing starch granule volume and surface area (Fig. S2) (Xu et al., 2016), a viewpoint further supported by the results of this study. In contrast, exogenous MGBG further suppressed starch granule development.

Amylopectin structure relies on the coordinated actions of starch synthases during biosynthesis (Hu et al., 2025). A and B1 are short chains, while B2 and B3 are long chains (Pang et al., 2024). DR decreased the proportion of short amylopectin chains and increased the proportion of long chains (Table 2) (Yang et al., 2024a). This is primarily because DR likely reduced GBSS activity, diminishing substrate competition for SBE. This allowed SBE greater opportunity to utilize available substrates for synthesizing or modifying long amylopectin chains, consequently increasing the proportion of long chains in the grains under DR conditions (Chen et al., 2025; Yang, Wang, et al., 2024). Exogenous Spd, resulted in higher proportions of A and B1 chains and lower proportions of B2 and B3 chains (Table 2), this is crucial for the physicochemical properties and digestive characteristics of star. Previous studies have indicated that neither water stress nor spermidine application alters the X-ray diffraction pattern of starch (Huo & Yang, 2022). Consistent with this, the crystalline diffraction profiles of starch in this study exhibited similar ‘A-type’ XRD patterns across treatments. However, relative crystallinity (RC) of starch increased significantly under DR influence, which can be attributed to the increased proportion of long chains B3 (Table 2), improved granule packing, and potentially reduced amylose content. A decrease in relative crystallinity was observed under DR + Spd conditions (Fig. 4 G), because the increased proportion of short amylopectin chains disrupts the regularity of molecular chain arrangement, leading to reduced starch crystallinity (Fig. 4 G) (Chen et al., 2025).

FTIR spectroscopy is sensitive to short-range ordered structures in starch. Spectral variations between starches from different treatments can be interpreted by changes in the short-range ordered structure present primarily in the external regions of starch granules (Man et al., 2014). Changes in the short-range molecular order of starch are reflected in the 800–1200 cm^{-1} spectral region, which corresponds mainly to C—C, C—O, and C-O-H stretching vibrations, as well as C-O-H bending vibrations (Yu et al., 2026). All treatments exhibited similar absorption bands (Fig. 4 E), indicating that severe DR and spermidine treatments did not form new chemical bonds or functional groups. The absorbance ratios at 1047/1022 cm^{-1} (R_1) and 1022/995 cm^{-1} (R_2) reflect the degree of short-range order and the arrangement of double helices within starch granules (Zhang et al., 2025). DR significantly increased the R_1 and R_2 ratios, indicating that DR enhanced the packing order of the short-range ordered structure in starch, consistent with the XRD analysis results (Fig. 4 G). However, exogenous Spd application reduced the R_1 and R_2 ratios under DR conditions (Fig. 4 H, Fig. 4 I). This is likely due to the synergistic effect of exogenous Spd (Shen et al., 2023), which introduced more short chains (Table 3) and disrupted the highly ordered structure to a certain extent, leading to molecular chain disintegration and helical structure distortion, ultimately damaging the short-range ordered structure of the starch (Li et al., 2025).

Table 4
Effects of exogenous spermidine on starch pasting properties of wheat under drought stress after anthesis.

Variety	Treatment	PV (cP)	TV (cP)	FV (cP)	BD (cP)	SB (cP)	PT (°C)
XN836	CK	3185.07 ± 67.89b	2825.37 ± 25.81c	3850.40 ± 43.56a	359.69 ± 5.97c	1025.03 ± 3.00a	84.55 ± 0.36d
	DR	3076.77 ± 16.87c	2713.67 ± 57.01d	3758.67 ± 27.61b	363.10 ± 9.80 cd	1045.33 ± 10.02a	86.68 ± 0.13bc
	DR + Spd	3362.08 ± 60.39a	3159.36 ± 97.64a	3932.00 ± 75.48a	202.70 ± 23.65f	772.70 ± 32.75e	81.92 ± 0.49e
	DR + MGBG	2981.03 ± 48.86 cd	2552.34 ± 41.52e	3533.77 ± 47.27c	428.69 ± 5.50b	981.47 ± 23.53b	86.60 ± 0.75c
XN979	CK	3188.01 ± 21.53b	2852.82 ± 37.99c	3693.33 ± 20.59b	335.19 ± 19.93d	840.67 ± 20.50d	85.03 ± 0.45d
	DR	3042.33 ± 2.51c	2546.86 ± 43.74e	3575.37 ± 30.16c	495.47 ± 16.56a	1028.51 ± 32.81a	87.72 ± 0.77ab
	DR + Spd	3222.20 ± 90.66b	2948.39 ± 44.44b	3733.23 ± 15.34b	273.81 ± 10.44e	784.83 ± 22.21e	84.58 ± 0.92d
	DR + MGBG	2904.83 ± 84.37d	2389.56 ± 51.20f	3274.00 ± 75.02d	515.27 ± 8.19a	884.44 ± 2.14c	88.20 ± 0.56a
	V	*	**	**	**	**	**
ANOVA	T	**	**	**	**	**	**
	V*T	ns	**	ns	**	**	*

Note: PT, Pasting temperature. PV, Peak viscosity. TV, Trough viscosity. BD, Breakdown. SB, Setback. FV, Final viscosity. PT, Gelatinization time. CK: 70%–75% soil relative humidity. DR: 35%–40% soil relative humidity. XN836: Xinong 836. XN979: Xinong 979. V: Variety. T: Treatment. V × T: Interaction of varieties and treatments. * and ** indicate significance at the $P < 0.05$ and 0.01 levels, respectively, ns: not significant ($P > 0.05$). All data represent means ± standard deviation of three replicates. Different lowercase letters represent significant differences, $P < 0.05$.

4.3. Spermidine improves the pasting and digestive properties of starch by optimizing its multi-scale structure in wheat under severe drought stress

Higher amylose content typically contributes to firmer and more rigid gels, consequently restricting granule swelling freedom, and vice versa. Under DR treatment, the swelling capacity of starch granules was restricted due to the decreased amylose content (Fig. 4) and the increased proportion of long amylopectin chains (Table 2), resulting in reduced swelling power and solubility (Fig. 4). Conversely, Spd treatment significantly enhanced the swelling power and solubility of starch by increasing the proportion of short chains and the proportion of small B-type granules (Table 1), as short chains are more readily hydrated and small granules possess a larger specific surface area (Shevkani et al., 2017).

The results demonstrated that DR significantly increased the onset (To), peak (Tp), and conclusion (Tc) gelatinization temperatures as well as ΔH. This can be attributed to its higher relative crystallinity (Fig. 4 G) and more stable double helix structure, as disrupting this ordered structure requires more energy (Toor et al., 2025). In contrast, Spd treatment reduced the energy and temperature required for gelatinization by decreasing molecular order (Table 3), leading to lower ΔH values and making the starch more readily gelatinizable (Wu et al., 2025). Exogenous MGBG exhibited the opposite trend.

The pasting properties of starch changed significantly under the synergistic effects of water status and spermidine (Table 4). Mondal et al. (2025) reported increased PV, TV, and FV under severe drought, whereas decreases were observed in this study, likely due to differences in drought duration and crop species (Lu et al., 2015). DR + Spd, however, increased PV, TV, and FV. The increased FV might be a consequence of the higher PV, which itself could result from the highest amylose content under DR + Spd (Fig. 3 E). Significant amylose leaching into the free water and higher granule swelling power (Fig. 4 C) facilitated the formation of a more viscous network upon cooling, thereby increasing FV (Singh et al., 2010).

A higher proportion of long chains facilitates the formation of longer double helices and more stable crystalline structures, requiring higher temperatures for dissociation (Rakita et al., 2023; Waterschoot et al., 2015). This study supports this conclusion, as the DR treatment, with its higher proportion of long chains (Table 2), promoted a more stable crystalline structure (Fig. 4 G), making the starch product more resistant

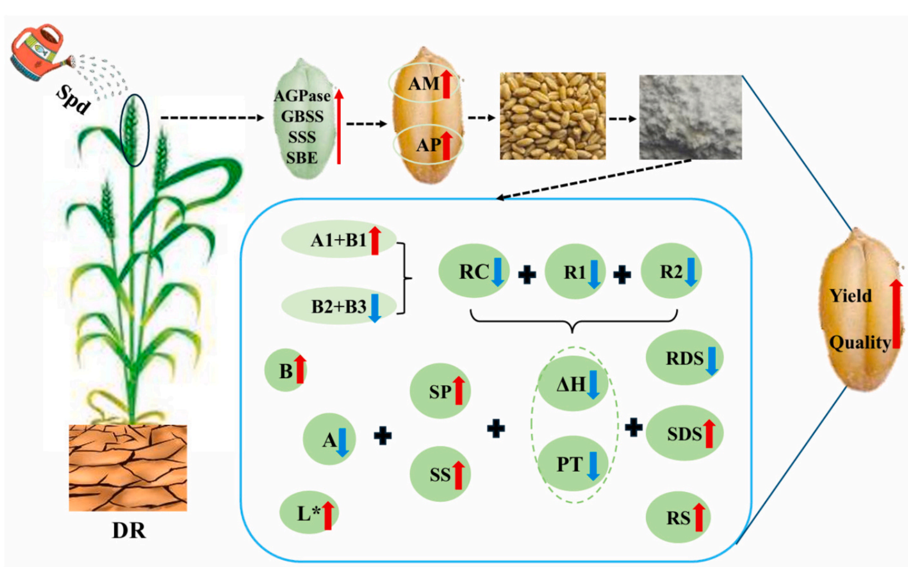

Fig. 6. Mechanism of spermidine increasing yield and starch quality of wheat under drought stress after post-anthesis.
Spd: Spermidine. DR:Drought stress. AGPase: ADP-glucose pyrophosphorylase. GBSS: Granule-bound starch synthase. SSS: Starch synthase. SBE: Starch branching enzyme. AM: Amylose starch content. AP: Amylopectin content. A1 + B1: Amylopectin short chain. B2 + B3: Amylopectin long chain. RC: Relative crystallinity. R_1: 1047/1022 cm^{-1}. R_2: 1022/995 cm^{-1}. B: B-type starch granules. A: A-type starch granules. L*: Brightness. SP: Swelling power. SS: Solubility. PT: Gelatinization temperature. ΔH: Gelatinization enthalpy. RDS: Rapidly digestible starch. SDS: Slow digestible starch. RS: Resistant starch.

to gelatinization and thus increasing the pasting temperature (Table 4). Fortunately, exogenous Spd appeared to mitigate the deterioration in starch product quality and texture induced by DR. Furthermore, the DR + Spd treatment resulted in the lowest setback (SB) value, indicating reduced short-term retrogradation tendency of the wheat starch paste. In other words, Spd likely inhibited the initial gel network formation from starch granules, delaying short-term staling (Kong et al., 2020). Superior taste and product texture are often associated with lower pasting temperature, higher peak viscosity, lower relative crystallinity, and lower gelatinization enthalpy (Chen et al., 2023). These results collectively indicate that exogenous Spd optimized the pasting properties of wheat starch under DR, making it more suitable for food processing applications requiring high viscosity and low retrogradation properties, such as soups and sauces (Wen et al., 2024).

The digestive properties of starch are crucial for its nutritional and health value. RDS is quickly absorbed in the gastrointestinal tract, leading to rapid increases in blood glucose levels. SDS and RS is beneficial for maintaining blood glucose stability and promoting intestinal health (Xu et al., 2019). In this study, DR increased RDS content while decreasing SDS and RS content (Fig. 5). Conversely, DR + Spd resulted in lower RDS and higher SDS and RS contents. This improvement might be linked to the increased proportion of B-type granules (Table 1), which typically exhibit fewer surface pores compared to A-type granules, potentially reducing the accessibility to hydrolytic enzymes (Liang et al., 2021). Increasing the SDS and RS content holds significant potential for developing low glycemic index (GI) and health-promoting foods, offering considerable benefits for human health (Gao et al., 2025; Liang et al., 2025).

5. Conclusion

This study demonstrates that exogenous spermidine effectively mitigates the adverse effects of DR on wheat by orchestrating a comprehensive improvement in starch yield and quality (Fig. 6). Physiologically, Spd promoted endosperm development and enhanced the activities of key starch-synthesizing enzymes, leading to increased amylose and amylopectin accumulation and higher grain yield. Structurally, Spd application optimized the multi-scale architecture of starch by increasing the proportion of B-type granules and short amylopectin chains, which consequently reduced starch relative crystallinity and molecular order. These structural modifications directly translated into superior functional properties, including lower gelatinization enthalpy and pasting temperature, and a nutritionally improved in vitro digestibility profile characterized by elevated levels of SDS and RS. Our findings elucidate the mechanism by which spermidine modulates starch multi-scale structure and functional properties under drought conditions, providing a theoretical foundation for improving wheat starch quality and developing wheat varieties with tailored functional characteristics for food industry applications.

CRediT authorship contribution statement

Jialu Wen: Writing – original draft, Conceptualization. **Jianli Liu:** Formal analysis. **Jianping Tang:** Investigation. **Ting Zou:** Investigation. **Aqing Gao:** Formal analysis. **Vinay Nangia:** Supervision. **Yang Liu:** Writing – review & editing, Resources, Funding acquisition.

Declaration of competing interest

The authors declare that they have no known competing financial interests or personal relationships that could have appeared to influence the work reported in this paper.

Acknowledgments

This research was supported by the National Key Research and Development Program of China (2024YFD2300205), the National Natural Science Foundation of China (32472229, 3227020750), Northwest A&F University Doctoral Candidates' Independent Innovation Research Project Funding (Z1050225014), and the Key Research and Development Program of Shaanxi (2024NC-ZDCYL-01-12).

Appendix A. Supplementary data

Supplementary data to this article can be found online at https://doi.org/10.1016/j.fochx.2026.103757.

Data availability

Data will be made available on request.

References

Chen, H. T., Luo, S. Q., Ma, Y., Jia, M. J., Cai, W., Liu, Y., … Zhang, W. Y. (2025). Brassinosteroids regulate amylose more sensitively than amylopectin: Essential for high-amylose premium rice. *Food Chemistry, 493*.
Chen, L., Deng, X. Y., Duan, H. X., Tan, X. M., Xie, X. B., Pan, X. H., … Zeng, Y. J. (2023). Water management can alleviate the deterioration of rice quality caused by high canopy humidity. *Agricultural Water Management, 289*.
Gao, L. C., Haesaert, G., Van Bockstaele, F., Vermeir, P., & Eeckhout, M. (2024). Effects of genotype, nitrogen, and Sulfur complex fertilization on the nutritional and technological characteristics of buckwheat flour. *Journal of Agricultural and Food Chemistry, 72*, 20603–20614.
Gao, L. C., Van Bockstaele, F., Haesaert, G., & Eeckhout, M. (2025). Recent advances in buckwheat starch: Structure, physicochemical properties, and the effects of genetic variation and fertilization. *Comprehensive Reviews in Food Science and Food Safety, 24*.
Gu, X. B., Xu, Y., Zhao, T. T., Du, Y. D., Zhang, Y. L., Tian, Y. Y., … Liu, Z. D. (2025). Nitrogen reduction with supplemental irrigation enhances yield by delaying leaf senescence and optimizing grain-filling process for ridge-furrow film mulching winter wheat. *Agricultural Water Management, 318*.
Hu, Y. Q., Zhang, Z. W., Li, X. Y., Yu, J., Chen, Y. L., & Bao, J. S. (2025). The functions of rice SSIIa alleles in starch biosynthesis modulated by the distinct genetic backgrounds. *Carbohydrate Polymers, 367*.
Huo, Z. G., & Yang, H. (2022). Application of exogenous 6-benzyladenine at the silking-stage improves the starch quality of waxy maize suffering from post-silking drought stress. *Starch-Stärke, 74*.
Kong, X. R., Zhu, Z. Y., Zhang, X. J., & Zhu, Y. M. (2020). Effects of cordyceps polysaccharides on pasting properties and in vitro starch digestibility of wheat starch. *Food Hydrocolloids, 102*.
Li, C., Li, C. Y., Zhang, R. Q., Liang, W., Kang, X. L., Jia, Y., & Liao, Y. C. (2015). Effects of drought on the morphological and physicochemical characteristics of starch granules in different elite wheat varieties. *Journal of Cereal Science, 66*, 66–73.
Li, G., Wei, J. L., Fu, K. Y., Yan, M., Liu, G. L., Qu, S. Y., … Li, C. (2025). Regulatory effects of organic compound L-glutamic acid on multi-scale structural characteristics of starch in high-quality wheat under post-anthesis drought stress. *Carbohydrate Polymers, 370*.
Li, G. G., Liang, Z. M., Li, Y. J., Liao, Y. C., & Liu, Y. (2020). Exogenous spermidine regulates starch synthesis and the antioxidant system to promote wheat grain filling under drought stress. *Acta Physiologiae Plantarum, 42*.
Li, G. T., & Zhu, F. (2018). Effect of high pressure on rheological and thermal properties of quinoa and maize starches. *Food Chemistry, 241*, 380–386.
Li, J., Li, G. G., Li, Z. Y., Li, J. Y., Xiao, J. K., Nangia, V., & Liu, Y. (2024). Spermidine alleviates drought-induced wheat floret degeneration by mitigating oxidative damage and maintaining energy homeostasis. *Crop Journal, 12*, 1765–1779.
Li, J., Liang, Z. M., Feng, J. Y., Hu, H. H., Nangia, V., Mo, F., & Liu, Y. (2024). Spermidine regulates wheat grain weight at high planting density by promoting the synthesis of sucrose and starch in inferior grains. *Physiologia Plantarum, 176*.
Li, J., Liang, Z. M., Li, Y. K., Wang, K. X., Nangia, V., Mo, F., & Liu, Y. (2024). Advantageous spike-to-stem competition for assimilates contributes to the reduction in grain number loss in wheat spikes under water deficit stress. *Agricultural Water Management, 292*.
Li, L. L., Mao, Z. Q., Wang, P., Cai, J., Zhou, Q., Zhong, Y. X., … Wang, X. (2025). Drought priming enhances wheat grain starch and protein quality under drought stress during grain filling. *Journal of Integrative Agriculture, 24*, 2888–2901.
Liang, W. X., Blennow, A., Herburger, K., Zhong, Y. Y., Wen, X. X., Liu, Y., & Liao, Y. C. (2021). Effects of supplemental irrigation on winter wheat starch structure and properties under ridge-furrow tillage and flat tillage. *Carbohydrate Polymers, 270*.
Liang, W. X., Herburger, K., Guo, K., Kirkensgaard, J. J. K., Hebelstrup, K. H., Persson, S., … Ding, L. (2025). Comparative analysis of supplemental irrigation effects on structure and digestion of normal and amylose-only barley starches. *Carbohydrate Polymers, 370*.
Liu, X. Y., Wang, M. T., Yan, J., Cheng, F., Liao, W., Xiao, Y. H., … Liang, Q. Z. (2025). Exogenous spermidine enhances drought resistance of mango seedlings by regulating physiological and biochemical metabolism. *Horticulturae, 11*.
Liu, Y., Gu, D. D., Wu, W., Wen, X. X., & Liao, Y. C. (2013). The relationship between polyamines and hormones in the regulation of wheat grain filling. *PLoS One, 8*.

Liu, Y., Liang, H. Y., Lv, X. K., Liu, D. D., Wen, X. X., & Liao, Y. C. (2016). Effect of polyamines on the grain filling of wheat under drought stress. *Plant Physiology and Biochemistry, 100*, 113–129.

Lu, D. L., Cai, X. M., Zhao, J. Y., Shen, X., & Lu, W. P. (2015). Effects of drought after pollination on grain yield and quality of fresh waxy maize. *Journal of the Science of Food and Agriculture, 95*, 210–215.

Lu, H. F., Wang, C. Y., Guo, T. C., Xie, Y. X., Feng, W., & Li, S. Y. (2014). Starch composition and its granules distribution in wheat grains in relation to post- anthesis high temperature and drought stress treatments. *Starch-starke, 66*, 419–428.

Man, J. M., Lin, L. S., Wang, Z. F., Wang, Y. P., Liu, Q. Q., & Wei, C. X. (2014). Different structures of heterogeneous starch granules from high-amylose Rice. *Journal of Agricultural and Food Chemistry, 62*, 11254–11263.

Mondal, K., Singh, R. K., & Dey, N. (2025). Combined drought and heat stress affect starch synthesis and grain quality-related traits during the grain-filling stage of rice (Oryza sativa L.). *Journal of the Science of Food and Agriculture, 105*(12), 8511–8524.

Ni, D. R., Tu, H. B., Yang, F., Yang, Y. B., Xu, Y., Zhang, B. H., … Kong, X. L. (2025). Impact of high-temperature daqu production on the starch structure of three wheat varieties with different granule size distribution. *Food Chemistry, 495*.

Pang, X. T., Zhang, D. M., Xue, H. B., Yao, D. P., Shen, H., Mou, B. H., … Bai, B. (2024). Effects of low field temperature on the physicochemical properties and fine structure stability of high-quality rice starch during the grain filling stage. *Foods, 13*.

Qiu, Y. L., Li, X., Fan, M., Tang, H. L., Zhang, S. X., Huang, W. H., … Wang, K. (2025). Modification of starch traits in commercial wheat through TaWaxy gene editing. *Carbohydrate Polymers, 368*.

Rakita, S., Torbica, A., Pezo, L., & Nikolic, I. (2023). Effect of climatic conditions on wheat starch granule size distribution, gelatinization and flour pasting properties. *Agronomy-Basel, 13*.

Ru, C., Hu, X. T., Wang, W. E., & Yan, H. (2024). Impact of nitrogen on photosynthesis, remobilization, yield, and efficiency in winter wheat under heat and drought stress. *Agricultural Water Management, 302*.

Shen, H. S., Yan, M. T., Liu, Y. L., Liu, X. Y., Ge, X. Z., Muratkhan, M., … Li, W. H. (2023). Multiscale structure-property relationships of oxidized wheat starch prepared assisted with electron beam irradiation. *International Journal of Biological Macromolecules, 235*.

Shevkani, K., Singh, N., Bajaj, R., & Kaur, A. (2017). Wheat starch production, structure, functionality and applications-a review. *International Journal of Food Science and Technology, 52*, 38–58.

Singh, S., Gupta, A. K., Gupta, S. K., & Kaur, N. (2010). Effect of sowing time on protein quality and starch pasting characteristics in wheat (Triticum aestivum L.) genotypes grown under irrigated and rain-fed conditions. *Food Chemistry, 122*, 559–565.

Toor, H. A., Chen, C. J., & Zhu, F. (2025). Relationship between physicochemical properties and molecular structure of barley starch with different size distributions. *Food Chemistry, 493*.

Van Hautegem, T., Takasaki, H., Lorenzo, C. D., Demuynck, K., Claeys, H., Villers, T., … Nelissen, H. (2025). Division zone activity determines the potential of drought-stressed maize leaves to resume growth after rehydration. *Plant, Cell & Environment, 48*, 1242–1258.

Waterschoot, J., Gomand, S. V., Fierens, E., & Delcour, J. A. (2015). Production, structure, physicochemical and functional properties of maize, cassava, wheat, potato and rice starches. *Starch-Starke, 67*, 14–29.

Wen, J. L., Feng, J. Y., Yao, J. F., Xiao, J. K., Nangia, V., Li, J., & Liu, Y. (2026). Moderate drought stress followed by re-watering enhances wheat starch biosynthesis, improving granule size distribution and physicochemical properties. *Carbohydrate Polymers, 374*.

Wen, J. L., Li, Z. Y., Yao, J. F., Wang, S., Liu, Y., & Liu, Y. (2024). The combined application of organic and inorganic fertilizers improved the quality of colored wheat by physicochemical properties and rheological characteristics of starch. *International Journal of Biological Macromolecules, 282*.

Wen, J. L., Tang, Y. Y., Li, J. Y., He, T. K., Xiao, J. K., Nangia, V., & Liu, Y. (2024). Effects of exogenous brassinosteroids on the starch structure, physicochemical properties and digestibility of wheat under high-temperature stress at the early grain-filling stage. *International Journal of Biological Macromolecules, 283*.

Wu, Z. W., She, Z. Y., Zhao, J. R., Yang, Y. R., Zhu, Z. Y., Zhao, Z. J., … Ma, T. T. (2025). Multi-scale structure provides new insights into the physicochemical and digestive behaviors of kiwifruit (*Actinidia* spp.) starch obtained from defective hard fruits. *Food Chemistry, 492*.

Xu, X. J., Luo, Z. G., Yang, Q. Y., Xiao, Z. G., & Lu, X. X. (2019). Effect of quinoa flour on baking performance, antioxidant properties and digestibility of wheat bread. *Food Chemistry, 294*, 87–95.

Xu, Y. J., Qiu, M. T., Li, Y. Y., Qian, X. Y., Gu, J. F., & Yang, J. C. (2016). Polyamines mediate the effect of post-anthesis soil drying on starch granule size distribution in wheat kernels. *Crop Journal, 4*, 444–458.

Yang, H., Wang, L. F., Guo, J., Li, G. H., & Lu, D. L. (2024). Degrees of post-silking water deficit alter the structural, pasting, and gelatinization properties of waxy maize starch. *Food and Energy Security, 13*.

Yang, J. Q., Wei, J. G., Ran, L. P., Liu, P. Y., Xiong, F., & Yu, X. R. (2024). The accumulation and properties of starch are associated with the development of nutrient transport tissues at grain positions in the spikelet of wheat. *International Journal of Biological Macromolecules, 282*.

Yang, W. B., Li, Y., Yin, Y. P., Jiang, W. W., Peng, D. L., Cui, Z. Y., … Wang, Z. L. (2014). Ethylene and spermidine in wheat grains in relation to starch content and granule size distribution under water deficit. *Journal of Integrative Agriculture, 13*, 2141–2153.

Yu, X. R., Li, B., Wang, L. L., Chen, X. Y., Wang, W. J., Gu, Y. J., … Xiong, F. (2016). Effect of drought stress on the development of endosperm starch granules and the composition and physicochemical properties of starches from soft and hard wheat. *Journal of the Science of Food and Agriculture, 96*, 2746–2754.

Yu, Z. T., Ma, N., Wei, F., Cui, H. X., Deng, J., Wang, R. C., … Wang, S. (2026). Structural determinants of physicochemical properties and digestibility of chestnut (*Castanea mollissima blume*) starches: Implications for functional and nutritional optimization. *Food Hydrocolloids, 171*.

Zhang, S. J., Wang, Z., Zhou, X. P., Song, Y., Wang, L. Y., Tian, H. L., … Zhang, X. R. (2025). Insights into the regulation mechanisms of dual hydrothermal treatment on the structure and digestive characteristics of A- and B-type wheat starch granules. *Food Research International, 200*.